2

A compaction model for melt transport in the Earth's asthenosphere. Part II: applications

A.C. Fowler
Mathematical Institute,
Oxford University,
24–29 St. Giles',
Oxford OX1 3LB, UK

Abstract

In this chapter, we summarize and simplify the model proposed in part I in a rational manner (avoiding *ad hoc* assumptions). We are then able to examine whether concepts that have been previously introduced in melt transport stand up to examination in the present context. We consider three topics: the existence of solitary waves ('magmons'), the idea of a compaction length, and the notion of magma accumulation at the base of the crust (or at the base of the lithosphere). We find that the practical relevance of solitary waves is questionable, at least in the form in which they have been studied. We find that the idea of compaction length has some merit, but that its appropriate description is both quantitatively and qualitatively different to those given previously. We find little to support the idea that magma can passively pond at the base of the lithosphere, but much to support the idea that partially molten zones fracture the lithosphere at their roofs.

Contents

Magma Transport and Storage. Edited by M.P. Ryan

Notation*

Many of the symbols are also used in part I, and can be found also in its 'Notation'. We do not include variables introduced in the appendices.

		Units
E	Young's modulus (52)	Pa
L	latent heat	J kg^{-1}
N	dimensionless parameter, O(1) (A24)	
Q	magma flux	m s^{-1}
St	Stefan number (26)	
S	melting rate	s^{-1}
T	temperature	K
T_m	melting temperature (24)	K
T_0	reference temperature	K
X	tortuosity coefficient	
a	grain diameter	m
c_p	specific heat	J kg^{-1} K^{-1}
d	depth of partial melt zone (17)	m
$\mathbf{g}$, g	gravity vector, scalar	m s^{-2}
k	thermal conductivity	W m^{-1} K^{-1}
(K_c), K	(critical) stress intensity factor (51)	Pa m$^{1/2}$
p_s	solid pressure	Pa
p_l	liquid pressure	Pa
p_0	reference pressure (15)	Pa
$[p]$	differential pressure scale (22)	Pa
p_e	effective (differential) pressure (49)	Pa
p^*	boundary value of subsolidus pressure (2)	Pa
r	shrinkage ratio, $=(\rho_s-\rho_l)/\rho_l$	
t	time	s
u^l, u^s	liquid and solid velocities	m s^{-1}
u_m	mantle velocity scale (17)	m s^{-1}
V_n	normal interfacial velocity (5)	m s^{-1}
v	liquid velocity relative to matrix (9)	m s^{-1}
$[v]$	liquid velocity scale (18)	m s^{-1}
w	dimensionless mantle velocity (35)	
y	vertical coordinate	m
$\tilde{y}$	modification to y for the bulk viscosity model (43)	

* The equation number is given in parentheses.

Γ	Clapeyron slope	K Pa^{-1}
$\Delta\rho$	density difference, $=\rho_s-\rho_l$	kg m^{-3}
Σ	critical stress for fracture (50)	Pa
β	thermal expansion coefficient	K^{-1}
γ	surface energy	Pa m
δ	dimensionless parameter (24)	
ε	dimensionless parameter (24)	
$\tilde{\varepsilon}$	dimensionless parameter	
η	shear viscosity of matrix	Pa s
η_m	mantle viscosity scale	Pa s
κ	permeability coefficient	m^3 s kg^{-1}
λ	dimensionless coefficient (24)	
μ_l	liquid viscosity	Pa s
ν, $\tilde{\nu}$	dimensionless coefficients (24)	
ρ	mixture density	kg m^{-3}
ρ_s, ρ_l	solid and liquid densities	kg m^{-3}
σ	normal stress (48)	Pa
τ_{ij}	matrix deviatoric stress tensor	Pa
τ_0	basic yield stress (50)	Pa
τ_f	yield stress (50)	Pa
τ_m	mantle deviatoric stress scale	Pa
ϕ	angle of internal friction (50)	
χ	melt mass fraction	
$[\chi]$	scale for χ (19)	
ψ	scaled differential pressure (21)	
ω	dimensionless parameter (24)	

1. Introduction

In the previous chapter, we discussed at some length the derivation of a consistent model for the porous transport of magma in the Earth's mantle. This model differs in some respects from previous models (McKenzie, 1984; Scott and Stevenson 1984,1986) but for the most part it is the same. However, there have been different applications of these models in the past, based on various simplifications. For example, Scott and Stevenson (1984,1986) and Richter and McKenzie (1984) consider the propagation of solitary waves in a compacting medium. This elegant idea has led to equally elegant laboratory experiments (Olson and Christensen, 1986; Scott, Stevenson and Whitehead, 1986), which graphically portray the basic theory. However, it is a moot point whether any of this has any relevance to the theory of a compacting, *reactive* medium, in which melting occurs. On the one hand there is the view that melting is a detail that may not seriously affect the dynamical behaviour of the compacting medium. On the other hand, it could be argued that in the Earth, the medium only *exists* by virtue of melting, and hence that it is meaningless to ignore it. It is, in fact, a straightforward matter to investigate which alternative is more appropriate. We do this in the section 'solitary waves and shock waves', after giving the appropriate model equations for the model and boundary conditions in section 2.

A basic result deduced by McKenzie (1984) was that there was a natural compaction length, denoted δ_c, beyond which compaction is essentially zero. Ribe (1985) refined this to include buoyancy effects, and showed that compaction typically occurred over a reduced compaction length $\delta_R \sim 10-100$ m. He concluded that compaction could essentially be ignored in the Earth. In fact, Ribe's analysis reproduced an older assumption of Turcotte and Ahern (1978), quantified by Ahern and Turcotte (1979) who obtained $\delta_R = 83$ m. In this respect, Ahern and Turcotte pre-empted the later analyses, and in addition, their results may be more applicable since they retain all the major physics of relevance (in particular, melting), and even the non-zero melt fraction necessary for percolation. Based on the present model (with its explicit compaction mechanism), we derive an expression for the 'compaction length' below; however, we also show that beyond this, compaction is reduced, but non-zero, a conclusion recently derived by Fowler (1989).

The process of melt extraction requires a mechanism for transmitting magma through the lithosphere without solidification, and the obvious mechanism is lithospheric fracture. The process is described by Nicolas and Jackson (1982) and Nicolas (1986), and a study of the dynamics of an upward propagating fracture was studied by Emerman, Turcotte and Spence (1986). Nicolas (1986) and also Fowler (1985) suggested that fracture of the partially molten medium will occur naturally when pore pressures are high; evidence for such fracturing exists in peridotite massifs, and the process is also observed in glacier ice.

Various authors have considered more complicated situations, notably two-dimensional flows (Ribe and Smooke, 1987; Spiegelman and McKenzie, 1987; Scott and Stevenson, 1989) at a ridge axis. Only the last of these includes melting in the dynamics: in this case the coupled 'circulation–percolation' model needs to be solved numerically. A further application (and one of interest) is to the geochemical signatures of erupted magmas. The inclusion of (trace element) chemistry in a model was offered by McKenzie (1984), and further discussed by McKenzie (1985a,b) and Richter (1986). Despite these contributions, no serious use of such applications can be made unless the process of ultimate transport to the Earth's surface is appropriately described. What is required, therefore, is a coupled model that describes both the percolative transport of magma below the lithosphere *and* the rapid ascent through dykes in the lithosphere (cf. Chapter 6); until such a model can be posed, it is premature to make inferences about chemical effects, and accordingly, we do not offer any such discussion in this paper.

2. Model, Boundary Conditions, Non-dimensionalization and Simplification

The model presented in chapter 1 consists of the equations (1–7), (9), (13–18), and is supplemented with boundary conditions (24), (26), (31), (35) and (45). We wish to simplify this by anticipating certain realistic approximations, which can in fact be justified by making the equations dimensionless.

First we anticipate that the melt fraction is small, that is

$$\chi \ll 1 \tag{1}$$

Ignoring terms of relative order χ in the equations leads to the equation set (19–22) in chapter 1. The associated boundary conditions are, approximately, (25) and (29), which is (without approximation)

$$p^* = p_s, \tag{2}$$

using equation (45); other boundary conditions are (30), (34) (ignoring deviatoric stresses), (35) and (45). For convenience, we reproduce the equations and boundary conditions here:

$$\chi_t + \nabla \cdot [\chi \boldsymbol{u}^1] = S \tag{3a}$$

$$\boldsymbol{u}^1 - \boldsymbol{u}^s = -\kappa\chi\nabla[p_1 + \rho_1 g y] \tag{3b}$$

$$p_s - p_1 = -(\eta_m/\chi)[\tau_m/|p_s - p_1|]^{n-1}\nabla\cdot\boldsymbol{u}^s \tag{3c}$$

$$\rho_s L S + \rho_s c_p \frac{dT}{dt} - \beta T\left[\frac{\rho_s}{\rho_1}\chi\left\{\frac{\partial p_1}{\partial t} + \boldsymbol{u}^1\cdot\nabla p_1\right\} + \left(\frac{1-\chi}{1+r\chi}\right)\left\{\frac{\partial p_s}{\partial t} + \boldsymbol{u}^s\cdot\nabla p_s\right\}\right] = k\nabla^2 T \tag{3d}$$

$$T = T_0 + \Gamma p_1 \tag{3e}$$

The matrix deformation equations (for circulation) are

$$\nabla\cdot\boldsymbol{u}^s = -\nabla\cdot[\chi(\boldsymbol{u}^1 - \boldsymbol{u}^s)] \tag{4a}$$

$$-\nabla p_s + \nabla\cdot\boldsymbol{\tau} + \nabla[(\rho_s/\rho_1)\chi(p_s - p_1)] + \rho\boldsymbol{g} = 0 \tag{4b}$$

$$\tau_{ij} = \eta\left(\frac{\partial u_s^i}{\partial x_j} + \frac{\partial u_s^j}{\partial x_i}\right) \tag{4c}$$

$$\eta \sim \eta_m[\tau_m/|p_s - p_1|]^{n-1} \tag{4d}$$

These are to be solved in a partially molten region D with a boundary ∂D and a unit outward normal $\mathbf{n}$. Let '+' denote the subsolidus side, and '−' the molten side of ∂D. The boundary conditions at ∂D are thus

$$u_n \approx u_n^s + \chi u_n^1 + r\chi V_n, \tag{5}$$

where V_n is the normal velocity of ∂D;

$$p^+ = p_s \tag{6a}$$

$$\tau_{nt}^+ = \tau_{nt}^- \tag{6b}$$

$$\rho\chi\left[L - p_1\left(\frac{1}{\rho_1} - \frac{1}{\rho_s}\right)\right](V_n - u_n^1) = \left[k\frac{\partial T}{\partial n}\right]_-^+ - p^+\chi(u_n^s + rV_n) \tag{6c}$$

$$[T]_-^+ = 0 \tag{6d}$$

$$\chi(p_s - p_1) = 0 \tag{6e}$$

(We do not write the equations in the cold zone explicitly, as they are of standard form.)

In order to simplify these equations further, we can use assumption (1), together with equation (4a), to obtain

$$\frac{d\chi}{dt_s} + \nabla\cdot[\chi\boldsymbol{v}] = S, \tag{7}$$

where

$$\boldsymbol{v} = \boldsymbol{u}^1 - \boldsymbol{u}^s, \quad d/dt_s = \partial/\partial t + \boldsymbol{u}^s\cdot\nabla \tag{8}$$

Darcy's law is

$$\boldsymbol{v} = -\kappa\chi\nabla(p_1 + \rho_1 g y) \tag{9}$$

and the compaction relation is

$$p_s - p_1 = (\eta_m/\chi)[\tau_m/|p_s - p_1|]^{n-1}\nabla\cdot[\chi\boldsymbol{v}] \tag{10}$$

We simplify the energy equation by anticipating that $p_1 \approx p_s$, and that each is nearly lithostatic:

$$p_1 \approx p_s \approx p_0 - \rho_s g y \tag{11}$$

Then, since $\beta T/\rho_1 c_p \Gamma \sim 0.2$ (Fowler, 1985), we find that equation (3d) simplifies uniformly to

$$\rho_s L S + \rho_s c_p \Gamma\, dp_1/dt - \beta T\{(1+r)\chi\boldsymbol{v} + \boldsymbol{u}^s\}\cdot\nabla p_s = k\nabla^2 T \tag{12}$$

where

$$\frac{d}{dt} = \frac{\partial}{\partial t} + \boldsymbol{u}\cdot\nabla, \quad \boldsymbol{u} = \boldsymbol{u}^s + \chi\boldsymbol{v} \tag{13}$$

A further important simplification can be made if we assume that

$$\boldsymbol{u}^s \gg \chi\boldsymbol{v} \tag{14}$$

that is to say, the mass transport of melt is much less than that of the matrix; in this case

$$\boldsymbol{u} \approx \boldsymbol{u}^s \tag{15}$$

and the advective terms in equation (12) correspond to advection by the matrix. This is an important simplification, since the melting term in equation (12) is essentially balanced (see below) by the heat advection term. If $\chi v > u$, the melt rate would depend on the melt fraction, and thus a positive feedback would occur, which might lead to local flow concentrations and thence to channelized flow; see also the discussion section. Here we ignore this possibility by anticipating equation (14).

The four equations (7), (9), (10) and (12) (equation (11) defining p_s) for the four variables $\chi, \boldsymbol{v}, S$ and p_1 are approximately accurate if assumption (1) holds. As we shall see, this is typically the case. They are coupled via the advective term involving $\boldsymbol{u}^s$ to the solid matrix flow, which is described by the biharmonic-type problem in equation (4).

Of the boundary conditions, (5) and (6a and b) apply to the external velocity field, if ∂D is known. If p_1 on ∂D is known, then boundary conditions (6c and d) determine both T and the location of ∂D via the Stefan condition. Hence only condition (6e) applies directly to the boundary value problem for the partial melt. In particular, if we suppose u^s is kinematically prescribed, then for a given location of ∂D, the equations (7), (9–12) with boundary condition (6e) form a closed system. If the set can be solved for a general boundary ∂D, then this boundary can be determined a posteriori by solving the external temperature problem.

For some applications, if the matrix flow field u^s is not significantly affected by the partial melt dynamics, it would seem reasonable to consider it kinematically prescribed. However, if for example ρ depends significantly on χ, then we would expect a significant coupling. This situation has been studied in detail by Scott and Stevenson (1989). Our approach here will be to consider the simple problem (u^s prescribed). In the concluding section we will examine how realistic this assumption is likely to be.

2.1. Non-dimensionalization

The system of equations for the partial melt is still quite complicated, but can be simplified further by anticipating what the important balance of terms is. The equations are, adopting the flux assumptions (14) and (15),

$$[\mathrm{d}\chi/\mathrm{d}t] + \nabla\cdot\{\chi v\} = S \tag{16a}$$

$$v = \kappa\chi\nabla\{(\rho_s - \rho_l)gy + [p_s - p_l]\} \tag{16b}$$

$$p_s - p_l = [(\eta_m/\chi)\{\tau_m/|p_s - p_l|\}^{n-1}\nabla\cdot\{\chi v\}] \tag{16c}$$

$$\rho_s LS + \rho_s c_p\Gamma\,\mathrm{d}p_l/\mathrm{d}t + [\beta(T_0 + \Gamma p_l)\rho_s g u_2^s] = [\Gamma k\nabla^2 p_l] \tag{16d}$$

and we anticipate that the terms in square brackets are (mostly) negligible: that is to say, melting is by pressure release, compaction is negligible, melt flows due to differential [illegible]oyancy, and melt advection with the matrix is negligible.

Rather than simply neglect the square-bracketed terms (which would not give the full picture anyway), we choose to justify the above statements by non-dimensionalizing the equations so as to preserve the indicated balances between the terms in equation (16). If d is a typical dimension (vertical, say) of the partial melt zone (remember, this really has to be det[illegible]mined a posteriori), then we choose

$$\chi v/d \sim S \tag{17a}$$

$$v \sim \kappa\chi(\Delta\rho)g \tag{17b}$$

$$p_l \sim \rho_s g d \tag{17c}$$

$$LS \sim c_p\Gamma\rho_s g u_m \tag{17d}$$

$$t \sim d/u_m \tag{17e}$$

where u_m is a typical matrix velocity scale, $\Delta\rho = \rho_s - \rho_l$, and recall that

$$\kappa = a^2/\mu_l X \tag{18}$$

where $X \sim 10^2$–10^3, a is grain size, μ_l is liquid viscosity. From equation (17), there follows the choice of liquid velocity and melt fraction scales:

$$\chi \sim [\chi] = \left[\frac{\rho_s\Gamma c_p u_m d}{L\kappa\Delta\rho}\right]^{1/2} \tag{19a}$$

$$v \sim [v] = \kappa\Delta\rho g[\chi] \tag{19b}$$

We now non-dimensionalize using these scales: thus, put

$$\chi = [\chi]\chi^*,\ v = [v]v^*,\ x = dx^*,\ t = (d/u_m)t^* \tag{20}$$

since $p_s = p_0 - \rho_s g y$, and we anticipate $p_l \approx p_s$, we put

$$p_l = p_s - [p]\psi \tag{21}$$

and we choose $[p]$ to balance equation (16c), that is,

$$[p] = \tau_m\{\eta_m[v]/\tau_m d\}^{1/n} \tag{22}$$

The dimensionless equations are thus

$$\delta\,\frac{\mathrm{d}\chi^*}{\mathrm{d}t^*} + \nabla^*\cdot(\chi^* v^*) = S^* \tag{23a}$$

$$v^* = \chi^*\nabla^*\{y^* + \nu\psi\} \tag{23b}$$

$$\chi^*|\psi|^{n-1}\psi = \nabla^*\cdot(\chi^* v^*) \tag{23c}$$

$$S^* - \frac{\mathrm{d}}{\mathrm{d}t^*}(y^* + \nu\psi) + [1 - \omega(y^* + \nu\psi)]u_2^{s*} = -\varepsilon\nabla^{*2}\psi \tag{23d}$$

wherein

$$\delta = u_m/[v] \tag{24a}$$

$$\nu = [p]/\Delta\rho g d \tag{24b}$$

$$\tilde{\nu} = [p]/\rho_s g d \tag{24c}$$

$$\lambda = \beta T_m/\rho_s c_p\Gamma \tag{24d}$$

$$\omega = \Gamma\rho_s g d/T_m \tag{24e}$$

$$\varepsilon = k[p]/d^2 c_p \rho_s^2 g u_m \tag{24f}$$

and T_m ($= T_0 + \Gamma p_0$) is the ambient melting temperature; u_2^{s*} is the dimensionless vertical matrix velocity, and since by equation (7), $u^* \approx u^{s*}$, then also $dy^*/dt^* \approx u_2^{s*}$.

The choice of scales is self-consistent provided that $\delta, \nu, \lambda, \omega, \varepsilon \ll 1$, and the assumptions behind equation (7) are justified if

$$\delta \ll 1 \quad (u^s \ll u^l) \tag{25}$$

and

$$St = L/c_p\Gamma\rho_s g d \gg 1 \quad (\chi u^l \ll u^s) \tag{26}$$

Since $\Delta T = \Gamma\rho_s g d$ is the drop in temperature across the partial melt zone, equation (26) defines the relevant Stefan number for the problem. Estimates of the parameters follow from the choices (Fowler, 1985; Kushiro 1986):

$g \sim 10\ \mathrm{m\,s^{-2}}$ (gravity)

$\rho_s \sim 3 \times 10^3\ \mathrm{kg\,m^{-3}}$ (matrix density)

$L \sim 3 \times 10^5\ \mathrm{J\,kg^{-1}}$ (latent heat)

$\Gamma \sim 10^{-7}\ \mathrm{K\,Pa^{-1}}$ ($10^{-2}\ \mathrm{K\,bar^{-1}}$) (Clapeyron slope)

$\beta \sim 3 \times 10^{-5}\ \mathrm{K^{-1}}$ (thermal expansion coefficient)

$T_m \sim 1500\ \mathrm{K}$ (ambient melting temperature)

$k/\rho_s c_p \sim 10^{-6}\ \mathrm{m^2\,s^{-1}}$ (thermal diffusivity)

$\tau_m \sim 10^6\ \mathrm{N\,m^{-2}}$ (10 bars) (ambient deviatoric stress)

$\eta_m \sim 10^{19}\ \mathrm{kg\,m^{-1}\,s^{-1}}$ (10^{20} poise) (ambient mantle viscosity)

$X \sim 10^3$ (tortuosity)

$a \sim 2 \times 10^{-3}\ \mathrm{m}$ (grain diameter)

$\mu_l \sim 1\ \mathrm{kg\,m^{-1}\,s^{-1}}$ (10 poise) (magma viscosity)

$c_p \sim 10^3\ \mathrm{J\,kg^{-1}\,K^{-1}}$ (specific heat)

$u_m \sim 10^{-9}\ \mathrm{m\,s^{-1}}$ ($3\ \mathrm{cm\,y^{-1}}$) (mantle velocity scale)

$d \sim 10^4\ \mathrm{m}$ (10 km) (typical depth of melting zone)

$\Delta\rho \sim 5 \times 10^2\ \mathrm{kg\,m^{-3}}$ (density difference) (27)

We find

$\kappa \sim 4 \times 10^{-9}\ \mathrm{m^3\,kg^{-1}\,s}$

$[\chi] \sim 2 \times 10^{-3}$

$[v] \sim 4 \times 10^{-8}\ \mathrm{m\,s^{-1}}$ ($1.3\ \mathrm{m\,y^{-1}}$)

thus

$$[\chi][v] \sim 0.8 \times 10^{-10}\ \mathrm{m\,s^{-1}} \tag{28}$$

which suggests that assumption (14) is appropriate. Moreover, note that $[\chi][v] = \rho_s\Gamma c_p g u_m d/L$, thus $[\chi][v]/u_m$ depends only on d. The positive feedback effect alluded to earlier therefore depends only on the depth of the partial melt region. The parameters are thus

$$\begin{aligned}&\delta \sim 0.025 \text{ (matrix velocity/melt velocity)}\\ &\mathrm{St} \sim 10\end{aligned} \tag{29}$$

in accordance with assumptions (25) and (26); we find

$$[p] \sim 40^{1/n} \times 10^6\ \mathrm{N\,m^{-2}} \tag{30}$$

Selecting $n = 3$,

$$[p] \sim 3 \times 10^6\ \mathrm{N\,m^{-2}} \text{ (30 bars)} \tag{31}$$

and then we obtain

$\nu \sim 0.06$ (compaction stress/buoyancy force)

$\bar{\nu} \sim 0.01$ (compaction stress/lithostatic pressure)

$\lambda \sim 0.15$ (adiabatic heat release/heat advection)

$\omega \sim 0.02$ (relative variation of melting temperature)

$\varepsilon \sim 0.001$ (heat conduction/heat advection) (32)

The values that we obtain for these parameters will obviously depend on circumstances. In particular, the value of $[p]$ depends on the choice of rheology for the compaction process, and the parameters ε, ν and $\bar{\nu}$ are proportional to it. The basic definition of $[p]$ is just $[p] = \eta_b[v]/d$, where η_b is the compaction viscosity. If we simply select $\eta_b \sim 10^{19}$ Pa s (10^{20} poise), then $[p] \sim 400$ bars, and it seems likely that non-linear stress dependence would be important. Alternatively, choosing $\eta_b \sim 10^{17}$ Pa s (10^{18} poise) would give $[p] \sim 4$ bars, and the constant viscosity might be reasonable.

We will base our analysis on the values given in (32), but recognize that in different circumstances, a value of $n = 1$ may be more appropriate, although the parameters ν, $\tilde{\nu}$ and ε are always likely to be small. We also see that all the assumptions on which the simplified model are based are realistic (although obviously, these parameters will vary with the circumstances). Furthermore, the smallness of the parameters in (32) suggests yet further approximations, as considered by Fowler (1989): we firstly summarize these results.

As we henceforth consider the dimensionless equations, it is convenient to omit the asterisks on the scaled variables. Eliminating S^* and v^*, they are

$$\delta \frac{d\chi}{dt} + \chi|\psi|^{n-1}\psi - \tilde{\nu}\frac{d\psi}{dt} - [1 - \lambda\{1 - \omega(y + \tilde{\nu}\psi)\}]u_2^s = -\varepsilon\nabla^2\psi$$

$$\chi|\psi|^{n-1}\psi = \nabla\cdot[\chi^2\nabla(y + \nu\psi)] \qquad (33)$$

with boundary condition

$$\chi\psi = 0 \text{ on } \partial D \qquad (34)$$

Although δ, ν, $\tilde{\nu}$ and ε are all small, their neglect may lead to singular perturbations. In the following sections, we consider certain applications in relation to such approximations.

3. Basic One-dimensional Solution, Compaction Length

A basic steady one-dimensional solution of equation (33) and boundary condition (34) was given by Fowler (1989), and we summarize his findings here (see the concluding part of section 3 of that paper). The steady one-dimensional problem is, taking a prescribed constant upwards matrix velocity $u = w$,

$$\delta w\chi_y + \chi|\psi|^{n-1}\psi - \tilde{\nu}w\psi_y - [1 - \lambda\{1 - \omega(y + \tilde{\nu}\psi)\}]w = -\varepsilon\psi_{yy} \qquad (35a)$$

$$\chi|\psi|^{n-1}\psi = [\chi^2(1 + \nu\psi_y)]_y \qquad (35b)$$

with

$$\chi\psi = 0 \text{ on } y = 0, 1 \qquad (36)$$

We suppose $\delta, \omega, \varepsilon, \nu, \tilde{\nu} \ll 1$ as in (32). Neglecting corresponding terms, we have

$$\chi|\psi|^{n-1}\psi = (1 - \lambda)w = 2\chi\chi_y \qquad (37)$$

whence

$$\chi = [(1 - \lambda)wy]^{1/2}, \ \psi = [(1 - \lambda)w/y]^{1/n} \qquad (38)$$

if we choose to satisfy $\chi = 0$ at $y = 0$. Evidently, there exist boundary layers at $y = 0$ and $y = 1$, in order to satisfy the boundary conditions.

These layers are analysed in Appendix A, with the following conclusions: there is a compaction zone of thickness $y \sim \nu^{2n/(2n+1)}$ near the base, where $\chi \sim \nu^{n/(2n+1)}$ and $\psi \sim \nu^{-1/(2n+1)}$. Beyond this, ψ and χ are O(1). Within this compaction zone, there is a further melting zone of thickness $y \sim \delta$, where χ jumps rapidly from zero to $O(\nu^{n/(2n+1)})$. At the base, the effective pressure ($\propto \psi$) is non-zero.

There is a further boundary layer at the top, $y = 1$, of thickness $O(\nu)$. The boundary layer structure is uniquely determined if

$$w > 4(1 - \lambda)(\varepsilon/\nu\delta)^2 \qquad (39)$$

a condition that may not be satisfied in practice. If condition (39) is violated, then boundary layer structures are not uniquely determined, and can be oscillatory (in space), although it is questionable whether such structures are physically realizable.

The physical implications of this analytical structure are these. The boundary layer (of thickness $\nu^{2n/(2n+1)}$) at the base corresponds to the compaction zone (cf. McKenzie, 1984). The thickness of this zone is, however, different to that given by McKenzie; moreover, beyond this zone, compaction continues to occur over the *whole* partially molten region. There is a *further* boundary layer at the top, *which is due to the imposition of the thermodynamic boundary condition (36)*, and within which the melt fraction increases significantly, and the compaction rate drops to zero.

We now try to compare these statements with the simpler notion of compaction in a system with zero melting (Ribe, 1985). The equations are derived from equation (24) by neglecting S^*, and omitting the energy equation. Then

$$\delta \frac{d\chi}{dt} + \chi|\psi|^{n-1}\psi = 0 \qquad (40a)$$

$$\chi|\psi|^{n-1}\psi = \nabla\cdot[\chi^2\nabla(y + \nu\psi)] \qquad (40b)$$

are the zero-melting replacements for equation (33). In one dimension, with matrix velocity $u = 1$, the steady problem is

$$\delta\chi_y + \chi\psi'' = 0 \qquad (41a)$$

$$\chi\psi'' = [\chi^2(1 + \nu\psi_y)]_y \qquad (41b)$$

The boundary conditions are rather vague, but we follow Ribe (1985) in prescribing $\chi = \chi_0$ at $y = 0$, and (essentially) $\psi = 0$ at $y = 1$. The outer solution is then just

$$\psi = 0, \ \chi = \text{constant} = \chi_\infty \tag{42}$$

The boundary layer is of thickness δ (or ν), so that compaction can occur over essentially the same thickness as when melting occurs. More specifically, we show in Appendix A that possible compaction zones are of thickness $O(\delta^{1/(n+1)}\nu^{n/(n+1)})$, but are not uniquely determined. This ill-posedness seems to be due to the vagueness of the prescribed boundary conditions. It is difficult to compare this result with that of Ribe (1985), since Ribe's compaction model is taken in the bulk viscosity form, and the matrix velocity therefore enters the problem. This follows from equation (21b) of part I; nevertheless, p_s is essentially lithostatic, as is assumed above. If we include the (small) viscous terms (in one dimension) then the term y in equation (40b) must be replaced by $\tilde{y}$, defined by

$$\tilde{y} = y + \tilde{\varepsilon}\frac{\partial}{\partial y}\left[\chi^2 \frac{\partial}{\partial y}\{\tilde{y} + \nu\psi\}\right] \tag{43}$$

where

$$\tilde{\varepsilon} = \eta_m \kappa [\chi]^2/d^2 \sim 10^{-3} \tag{44}$$

using the values in (27). It is debatable whether the inclusion of this term has practical significance.

We conclude the following: firstly, there is a small difference between the bulk-viscosity model and that used here, since in the former, the matrix velocity enters explicitly into the problem. The fact that $\tilde{\varepsilon}$ in equation (44) is small *suggests* that this is a small difference, but it *may* be a singular approximation. Secondly if melting is ignored in the present model, it seems difficult to pose a meaningful problem properly: the far-field melt fraction is unconstrained.

At any rate, what does seem clear is that the size and form of a compaction zone is rather dependent on whether melting is included, and what boundary conditions are applied. Simple models for compaction therefore need to be treated with some care.

4. Solitary Waves and Shock Waves

The idea that solitary waves, dubbed 'magmons', could propagate through compacting media was originated by Scott and Stevenson (1984,1986) and Richter and McKenzie (1984). It was later demonstrated that the governing equations applied to a laboratory analogue experiment (Scott, Stevenson and Whitehead, 1986). More complicated situations were also considered, for example, cylindrically symmetric waves (Scott, Stevenson and Whitehead, 1986) and the inclusion of background (matrix) circulation (Scott, 1988). The literature on solitary waves in partially molten rock is suitably cautious in drawing tentative conclusions concerning geophysical applications, such as episodicity of surface volcanism. One way to examine the applicability of the wave models is to see whether they are likely to have quantitative accuracy, and in particular to study the effect of including terms that are neglected. The principal assumption used in deriving the wave equation in compacting media is to ignore melting. Thus the basic equations in the partially molten zone are just (16a–c) (ignoring the energy equation (16d)), and we put $S = 0$ in (16a). We now trace the consequence of this assumption. We retain the same non-dimensionalization, though now, with $S = 0$, we choose the melt scale $[\chi]$ arbitrarily. With $[\chi] \sim 1\%$, we obtain equation (23), with $S^* = 0$ and not (23d), and the same estimates of the parameters.

Our equations in this form are then

$$\delta \frac{d\chi}{dt} + \nabla\cdot(\chi v) = 0 \tag{45a}$$

$$v = \chi\nabla[y + \nu\psi] \tag{45b}$$

$$\chi|\psi|^{n-1}\psi = \nabla\cdot(\chi v) \tag{45c}$$

and these are directly comparable to equations (3) and (4) of Scott and Stevenson (1984). In Appendix B we review the results for equation (45), and compare these with equivalent results when melting is included on the right-hand side of equation (45a) as a term S, approximately given (see equation (33)) by

$$S \approx (1-\lambda)u\dot{z} + \nu\frac{d\psi}{dt} \tag{46}$$

The conclusions we draw are as follows.

(i) When $S = 0$ (zero melting), solitary waves such as those treated by Scott and Stevenson (1986) or Whitehead and Helfrich (1986) can propagate. Their speed is $O(1/\delta)$, so that these waves move rapidly through the system.

(ii) When $S \neq 0$, then a similar analysis to that of Whitehead and Helfrich shows that (when

$M = 0$, see Appendix B) waves move through the system at a non-constant speed of $O(1/\delta)$, and specifically at speed $2z^{1/2}/\delta$, where now z is the vertical coordinate (and $z = 0$ at the base of the melt zone). Thus waves start sluggishly, and then accelerate. Their amplitude decays like $1/z^{1/2}$. On a long time-scale, they evolve according to a non-linear evolution equation that includes non-linearity and dispersion (the solitary wave ingredients), and also diffusion. Therefore such waves will tend to degrade. However, in practice the waves pass through the system in time of $O(\delta)$, so that the non-linear evolution is in practice irrelevant.

(iii) The above result follows from including melting via the advection of sensible heat, but neglecting the Clapeyron relation that relates T to p_l. If this also is included, then the basic (linear) propagation problem is that of equation (B12) (with $M \neq 0$); and it seems that this linear equation will have wave-like solutions that grow unstably as they propagate. However, this may reflect the non-linear hyperbolic nature of the problem, with a propensity to form shocks.

(iv) In fact, the leading order problem for dynamic disturbances is just equation (B19). When $M = 0$ (as in (ii)), most perturbations to the steady state form shocks, and thus in practice, waves would tend to be step-like rather than solitary. When $N \neq 0$, no immediate conclusion can be made.

(v) For the mantle, the short time-scale suggests that any disturbances will wash out rapidly, without significant evolution. However, since external thermal disturbances (e.g., mantle plumes) will typically fluctuate on much longer time-scales, one would in that case expect the partial melt region to respond quasi-statically. This then suggests that for most purposes, one may treat the melt zone (in the present model) as quasi-stationary. This, of course, excludes the possibilities when $M \neq 0$ in equation (B19). Alternatively, chemical inhomogeneity could lead to transient solutions.

5. Fracture and Segregation

There can be little doubt that transport of basaltic magma through the lithosphere and crust takes place by rapid ($O(\mathrm{m\,s^{-1}})$) flow through conduits that originate as fluid-assisted fractures. Abundant testimony is provided by the commonplace observations of dykes and veins in surface rocks, and, at a deeper level, from the migration of earthquake swarms associated with active conduit regions beneath Hawaii (Ryan, Koyanagi and Fiske, 1981; Ryan, 1988). Furthermore, rapid transport is required if magma is not simply to solidify on its way to the surface. This difficulty appears insurmountable for the idea that buoyant diapirs can rise all the way through the lithosphere (e.g., Marsh, 1978). There are then two problems to address: firstly, given that flow at great depth is by percolation through a compacting, porous medium, can one predict when fracturing should occur? Secondly, if the flow evolves from a slow percolation to a more rapid ascent along dykes, can one model this process in a realistic way?

In this section, we address the first of these topics; the second is a subject for further work, but an important one, since little of any substance can be said about observed surface rocks (chemistry, volume, etc.) unless some description of this process is given. Despite this, there has been little effort so far to study this problem, and most authors implicitly suppose that the predicted upflow of magma in the percolation zone all appears at the surface (e.g., McKenzie, 1984; Richter, 1986; Spiegelman and McKenzie, 1987; Ribe and Smooke, 1987). Another possibility would be that none of it does, and that freezing occurs at the top of the partial melt zone. Here we attempt to chart the possibilities.

The basic physics of the theory of (quasi-static) fracture of an elastic medium is reviewed by Shaw (1980) and Spera (1980) in the context of magmatic transport, and the general theory of 'stress corrosion' fracture, as applied to ceramics (in particular), is reviewed by Anderson and Grew (1977). The propagation of fluid-assisted fractures through the lithosphere has been analysed by Emerman, Turcotte and Spence (1986), and Nicolas and Jackson (1982) and Nicolas (1986) give a detailed description of the processes that are thought to operate. In particular, Nicolas (1986, figure 5) shows the development from an interconnected percolative regime into an interconnected fractured regime, and Sleep (1988) has considered the process in some detail theoretically. We now discuss why such a situation should develop.

At the phenomenological level, one might expect rock at depths of > 50 km to be ductile and not brittle. This is, of course, the case for subsolidus rocks, although even there the behaviour depends on the stress. However, one cannot draw the same conclusion for partially molten rocks. From the thermodynamic (energetic) point of view, rocks fracture when they can lower their free energy by converting elastic strain energy to surface energy, and this is the idea behind the Griffith fracture criterion. In this thermodynamic sense, partially molten rock is *already fractured*, in so far as it has converted sensible heat to surface energy by melting. Thus, fracturing of partially molten rock can be viewed simply as a modification of the melt geometry.

There are also some analogies. In the phenomenon of frost heave (Miller, 1980; O'Neill and Miller, 1985), soil water flows upwards through a partially frozen 'fringe'. As it does so, the effective pressure (which is the soil intergranular pressure) may decrease to zero. When this happens, there is no longer any cohesion between the soil grains, which may then spontaneously separate; water flows into the gap, and freezes to form ice lenses, which are often (though not always) roughly horizontal. A different analogy is that of the formation of crevasses in glaciers. Alpine glaciers are temperate (i.e., partially molten) and the wet ice commonly fractures, rather like jelly. Icebergs calve in this way.

In the presence of deviatoric stress, a criterion for fracture can be written as

$$\tau > \tau_f(\sigma) \tag{47}$$

where

$$\sigma = p_e + \tau_1 \cos 2\alpha, \quad \tau = \tau_1 \sin 2\alpha \tag{48}$$

σ and τ define the normal and shear stresses on the Mohr circle, p_e is the effective pressure

$$p_e = p_s - p_l \tag{49}$$

and $\tau_1 > 0$ is the maximum principal extensional deviatoric normal stress, and α is the angle between the failure plane and the minimum principal effective stress component. Failure occurs if, for some α, τ reaches $\tau_f(\sigma)$. Two commonly used criteria are

$$\tau_f(\sigma) = \tau_0 + \sigma \tan \phi \text{ (Coulomb)} \tag{50a}$$

$$\tau_f(\sigma) = 2\Sigma(1 + \sigma/\Sigma)^{1/2} \text{ (Griffith)} \tag{50b}$$

If there is no deviatoric stress, the failure criterion is simply $p_e \leqslant -\tau_0/\tan \phi$ (Coulomb) or $p_e \leqslant -\Sigma$ (Griffith). Shaw (1980, figure 5) estimates $\Sigma \sim 10$ bars, to within an order of magnitude, but as a deduction from plate tectonic models, which is likely to be unreliable. Also, he identifies this value of Σ with a yield stress (for slip), which is not necessarily the same.

A different idea uses the stress intensity factor (Rudnicki, 1980). For a crack of length l subjected to a differential stress $\Delta\tau$, the stress intensity factor is

$$K \sim l^{1/2}\Delta\tau \tag{51}$$

and subcritical cracks propagate if $K > K_c$. For subsolidus rocks, typical values are $K_c \sim 10^2$ bar m$^{1/2}$. Alternatively, for intergranular stress differences $\Delta\tau \sim 10$ bars, and a grain size $l \sim a \sim 2 \times 10^{-3}$ m (see equation (28)), we obtain an estimate of $K \sim 1$ bar m$^{1/2}$. However, it seems extremely unlikely that values of K_c as high as 10^2 bar m$^{1/2}$ should apply to partially molten material.

In discussing fracture, it is important to draw a fundamental distinction between melting and solidifying mixtures. Crystal mushes (e.g., in magma chambers) solidify 'incoherently', that is, so that the liquid will wet most of the grains until the melt fraction is very small; this is because crystal nucleation and growth are randomly dispersed and oriented. For such a mixture (and for others, e.g., saturated soil or till (Boulton and Hindmarsh, 1987), a yield stress is a barrier to slip: the yield stress is essentially static friction between grains; when this is exceeded, large-scale deformation can occur. However, partially molten rock (with dihedral angle less than 60°) has melt confined to three-grain intersections. Thus, the process of fracturing such a medium occurs by melt invading grain boundaries, and this is analogous to the ordinary fracture of a solid, except that the intergranular boundary is a surface that is naturally weak, due to the elevated temperature.

We expect fracture in partially molten rock to be ductile fracture (Broek, 1986), since at such elevated temperatures the solid grains can deform viscously to accommodate the propagation. The Griffith criterion (which is identical to the stress intensity criterion for brittle fracture) suggests that fracture will occur when the stored elastic energy is sufficient to form the new surface energy associated with a propagating crack. The stored energy per grain is $\sim \sigma^2 a^3/E$, where E is the Young's modulus, σ is the differential stress, and a is grain diameter. Because of the viscous creep

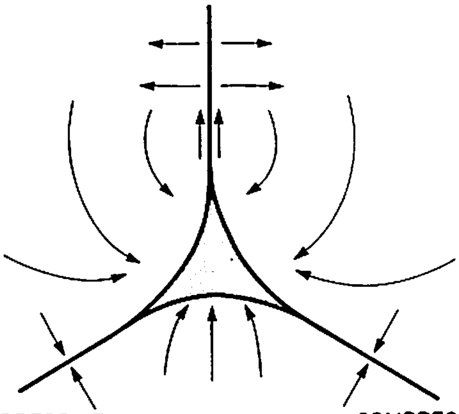

Figure 1. Schematic creep directions at the onset of grain boundary fracture at a three-grain intersection

behaviour (no yield stress), energy associated with wetting two-grain interfaces is surface energy, which per grain is $\sim \gamma a^2$, where γ is surface energy. A Griffith-like criterion (Sleep, 1988) is thus (with $\sigma < 0$)

$$|\sigma| \gtrsim (E\gamma/a)^{1/2} \quad (52)$$

and is analogous to a stress intensity criterion, with $K_c \sim (E\gamma)^{1/2}$. With $E \sim 10^6$ bars, $\gamma \sim 2 \times 10^{-7}$ bar m, $a \sim 2 \times 10^{-3}$, then equation (52) gives $|\sigma| \gtrsim 10$ bars. In reality, subcritical growth is likely, so that a lower value may be appropriate.

Fracture will occur normal to the minimum compressive principal stress, $-\sigma_m$ say, in the matrix (see Figure 1), and then the appropriate definition of σ is

$$\sigma = p_l + \sigma_m \quad (53)$$

With τ_l (> 0) as the maximum principal extensional deviatoric stress, this criterion is identical to equations (47) and (48) with $\alpha = \pi/2$, and $\tau_f[(E\gamma/a)^{1/2}] = 0$. This corresponds to the Griffith envelope (equation (50b)) when

$$\Sigma \sim (E\gamma/a)^{1/2} \quad (54)$$

and $p_e \approx 0$. In fact, if $p_e \sim [p] \sim 30$ bars, this fracture criterion can be met only near the top of the partially molten zone, where $p_e \to 0$.

The simple criterion that results from this discussion is that intergranular fracture can occur if equation (52) applies, that is, if

$$p_s - p_l < \tau_l - \Sigma \quad (55)$$

where τ_l is the largest deviatoric extensional stress. More complicated criteria could be postulated, but there seems little point. Fracture is normal to the direction of τ_l. It may be recalled that we suggested in part I that the viscosity in the partially molten region (given by equation (15a)) would plausibly be significantly lower than the surrounding subsolidus mantle, and that on that account the partial melt zone would behave much like a bubble (and, in particular, would not be able to sustain much deviatoric stress). In fact, this should apply where $p_s - p_l > \tau_m$, but where $p_s - p_l \to 0$, the viscosity increases again to ambient mantle values; this happens precisely in the boundary layer at the lithosphere base (see section 3), and we thus suggest that this boundary layer will be like a viscous skin at the top of the less viscous partial melt zone, and hence that it will act as a kind of stress guide: that is, stresses will increase with y as the viscous skin is traversed. A similar phenomenon occurs in variable viscosity convection (Fowler, 1984). We then have τ_l increasing as p_e decreases, and if equation (55) can be satisfied, it should be at the top of the partial melt zone.

Evidently, fracture will not occur if $\tau_l < \Sigma$. For the situation envisaged here (upwelling mantle flow), τ_l will be horizontal, and thus fractures will be directed vertically upwards, provided the rock is being pulled sideways fast enough. If $\Sigma \sim 10$ bars, then, since this is also a typical estimate of mantle deviatoric stress, fracture to upwardly propagating dykes seems to be a realistic possibility.

Another mechanism for the initiation of dykes has been suggested in his review of this paper by David Stevenson (see also Sleep (1988)). A local region of increased melt fraction attracts melt by percolation, and thus a horizontally uniform upwelling may be unstable to formation of channelized flow; presumably, if this instability is not limited in its development, the 'channels' 'become' xenocryst-laden dykes, and can propagate into the lithosphere. This idea is certainly worthy of further study. It is akin to the arborescent tendencies of subglacial drainage channels (Röthlisberger 1972), as can be seen from the following crude discussion. From equation (A4) of Appendix A, we have the magma flux $Q \sim \chi v \sim \chi^2 \partial\psi/\partial y \sim y^{-1/2n} \sim \psi$. Thus Q decreases as p_l increases (ψ decreases), which is precisely the requirement for flow concentration into an arborescent network. The instability of Scott and Stevenson (1986) may be related to this. *If* this idea is correct, there is very little problem in initiating dykes, but in fact the whole magma transport dynamics would need rethinking.

Setting aside this possibility, we therefore predict that fracture will essentially occur at the top of the molten zone, where the magma would otherwise solidify. Veins and gashes form, and consequently the flow accumulates in these veins. Larger flow rates require smaller pressure drops, and thus there is also a natural mechanism whereby arborescent channels can form in the lithosphere (Röthlisberger, 1972). Provided such channels become large enough, the Peclet number for the flow will become large, and in that case fractures may propagate unhindered through the lithosphere, since at large Peclet number, they will deliver heat *to* the surrounding country rock (they will *not* solidify).

We expect that fractures form perpendicular to the minimum compressive stress. At spreading centres and hot spots, the mantle flow is laterally extensional, and therefore we expect the fracture to be vertical. Conversely, in convergent regions, we should expect lateral sill-like ponding of magma to occur (analogously to frost heave). In this case, however, there is nothing to prevent the magma freezing, and we should expect volcanism to be largely absent.

6. Conclusions

Partial melting in the mantle is a complicated process. Nevertheless, simple models may give good results, but one needs to be aware of the complications. This chapter aims to critically discuss some of these. In particular, we have discussed the implications when critically important parts of the overall process are omitted from the analysis.

6.1. If melting is ignored

In this case, consideration of dynamic perturbations leads to the conclusion that solitary waves may exist. This attractive theory may be linked tentatively to ideas of episodicity in volcanism. Indeed, when melting is included in a realistic way, the theory is fairly resilient, though one expects waves to decay diffusively. However, the practical relevance of such waves is questionable, given their rapid time-scale of propagation. It seems unlikely that the partially molten region would respond other than quasi-statically to perturbations (such as mantle plumes).

6.2. If compaction is modelled as a bulk viscosity

Although the same equations result as from choosing a two-pressure model, some distinction occurs through the boundary conditions. We find here a 'compaction zone', to be sure, but one in which effective pressure drops only slightly—and not to zero. The physical significance of this zone is therefore diminished.

6.3. If thermodynamics is ignored

Apart from losing the energy equation if melting is ignored, few authors have considered the possibility of melt refreezing at the base of the lithosphere. One can simply assume that it all gets through to the surface (via conduits, for example), but this then ignores a physical process of major importance. Furthermore, a two-pressure model requires a critical consideration of melt-pressure boundary conditions. Satisfaction of these boundary conditions requires the existence of boundary layers at both the top and the bottom of the partially molten zone. In particular, the effective pressure jumps to zero near the top. Nor is the mathematical structure of these boundary layers trivial to resolve: there remain uncertainties about the solution, which are described in Appendix A.

6.4. If fracture is ignored

It is natural to do so if the effective pressures are not considered, but analogues with other similar systems (solidifying magma and freezing soil) strongly suggests that fracture can realistically occur at the top of the percolative zone. Then the model must be changed, and this seems to be a major challenge for the future. It renders current models inapplicable in realistic attempts to describe adequately the total process. So also would the channeling of the melt transport via an arborescent network.

6.5. If circulation is ignored

Most of the present discussion has considered melt dynamics uncoupled from the larger scale mantle circulation. That is, equation (3) is considered with u^s prescribed kinematically. In reality, u^s is determined from equation (4), and will be affected considerably by two features. Firstly, if solid state creep depends non-linearly on stress, then the partial melt viscosity ought to be significantly lower than the subsolidus mantle viscosity. If $\tau_m \sim 10$ bars, $p_s - p_l \sim 30$ bars and $n = 3$, then the ratio is ~ 10. The partial melt zone is therefore 'softer'. Secondly, the melting of realistic mantle rocks can yield a residue (e.g., harzburgite) that is *lighter* than the parent rock. If mantle rocks undergo a significant degree of melting, therefore, then the matrix density can be changed significantly. Certainly this change is enough to provide an important buoyancy term in the circulatory flow. This coupling has been examined numerically by Scott and Stevenson (1989), and has important consequences for the flow. The simple corner flow circulation is distorted and interacts in a complicated way with the melting process.

If the viscosity is low enough, and the melting induced buoyancy is large enough, the partially molten domain will tend to develop its own circulatory convection cell. This is indeed indicated by Scott and Stevenson's (1989) results. Now the only effective coupling of u^s to the partial melt dynamics is in the adiabatic heating. Thus from equation (34),

$$\chi\,|\psi|^{n-1}\psi \sim 2\chi\chi_y - (1-\lambda)u_2^s \qquad (56)$$

Now *if* we anticipate $\chi = 0$ at the lower boundary, then we require $u_2^s > 0$ there. Hence any melt-buoyancy circulation must be no more than comparable to the mantle circulation. If the partially molten viscosity is low enough, and/or the melt buoyancy is large enough, this seems difficult, and a possibility is that buoyancy (and most melting) is confined to a thin upwelling region, with a broader, slower return flow. This is relatively consistent with Scott and Stevenson's results.

In closing, it is to be hoped that the critique offered here may be seen in a constructive light, and that it may help in identifying the directions that will be important in future work.

Acknowledgements

For helpful reviews, I am grateful to David Stevenson, Norm Sleep, Michael Ryan and David Scott.

Appendix A: Compaction

We consider the equations (35a) and (35b) with $\omega = 0$, and assuming $\psi > 0$:

$$\delta w\chi_y + \chi\psi^n - \tilde{\nu} w\psi_y - (1-\lambda)w + \varepsilon\psi_{yy} = 0 \qquad (A1a)$$

$$\chi\psi^n = [\chi^2(1+\nu\psi_y)]_y \qquad (A1b)$$

with

$$\chi\psi = 0 \text{ on } y = 0, 1 \qquad (A2)$$

We suppose δ, ν, $\tilde{\nu}$, $\varepsilon \ll 1$, specifically

$$\delta \sim 0.025,\ \nu \sim 0.06,\ \tilde{\nu} \sim 0.01,\ \varepsilon \sim 0.001 \qquad (A3)$$

The outer solution, neglecting $O(\delta, \varepsilon, \nu)$, is thus

$$\chi \sim [(1-\lambda)wy]^{1/2},\ \psi \sim [(1-\lambda)w/y]^{1/2n} \qquad (A4)$$

(we assume it satisfies $\chi = 0$ at $y = 0$, as the alternative does not seem to work).

Boundary layer at $y = 0$

There is a *compaction zone* in which

$$y \sim \sigma \equiv \nu^{2n/(2n+1)} \qquad (A5a)$$

$$\psi \sim 1/\sigma^{1/2n} \qquad (A5b)$$

$$\chi \sim \sigma^{1/2} \qquad (A5c)$$

Rescaling the variables as indicated, and denoting the boundary layer variables by Y, Ψ, X, gives the leading order problem

$$X\Psi^n \sim (1-\lambda)w \qquad (A6a)$$

$$X^2(1+\Psi_Y) \sim (1-\lambda)wY \qquad (A6b)$$

on integrating and matching to (A4): we assume $\delta \ll \sigma^{1/2}$, $\nu \ll \sigma^{(1/2)+1/2n}$, $\varepsilon \ll \sigma^{1+(1/2n)}$. Thus Ψ satisfies

$$\Psi_Y = \Psi^{2n}Y/[(1-\lambda)w] - 1 \qquad (A7)$$

and $\Psi \sim [(1-\lambda)w/Y]^{1/2n}$ as $Y \to \infty$. The solutions of equation (A7) vary monotonically with $\Psi_0 = \Psi|_{Y=0}$. Obviously, if Ψ_0 is large, Ψ crosses $\Psi_Y = 0$ at finite Y, whereas if Ψ_0 is small, $\Psi = 0$ for finite Y. There is clearly a unique value $\Psi_0 = \Psi_0^*$

such that equation (A7) has the correct behaviour as $Y \to \infty$. Then as $Y \to 0$, Ψ is finite, but now $X \neq 0$ at $Y = 0$. We require a further 'melting' layer, in which X (i.e., χ) drops to zero.

Melting layer

In this,

$$Y \sim \bar{\delta} = \delta/\sigma^{1/2}, \text{ i.e., } Y = \bar{\delta}Z \qquad \text{(A8a)}$$

$$\Psi = \Psi_0^* - \bar{\delta}Z + \bar{\delta}^2\psi_m \qquad \text{(A8b)}$$

then

$$X\Psi_0^{*n} \sim [X^2\psi_{mZ}]_Z \qquad \text{(A9a)}$$

$$wX_Z - (1-\lambda)w + X\Psi_0^{*n} \sim 0 \qquad \text{(A9b)}$$

whence

$$X \sim [(1-\lambda)w/\Psi_0^{*n}][1 - \exp\{-\Psi_0^{*n}Z/w\}] \qquad \text{(A10)}$$

The schematic structure of the composite boundary layer is shown in Figure A1.

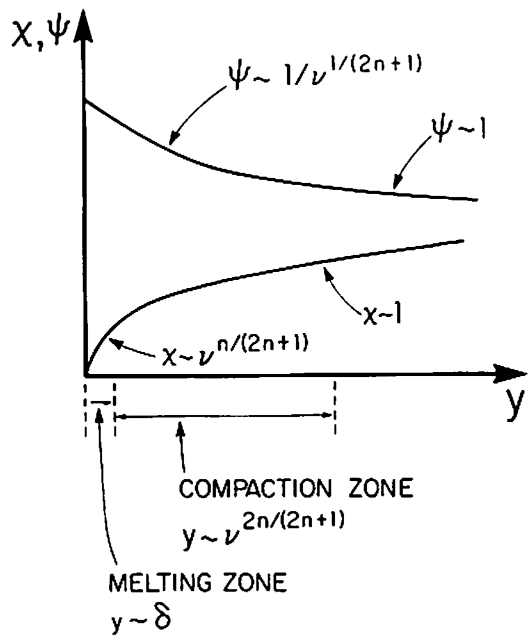

Figure A1. Schematic variation of ψ and χ with y near $y = 0$. There is a thin compaction zone (if $\nu \sim 0.06$, $d = 10$ km, $n = 3$, of thickness $\sim$ 1 km) within which the differential pressure drops mildly from O(50) bars to O(30) bars. Beyond this zone, compaction continues to occur as the melt fraction increases. Within the compaction zone, a slightly thinner (O(0.5) km) melting zone causes an initial rapid rise of the melt fraction from zero to O(1%)

Boundary layer at $y = 1$

Here we write

$$\varepsilon = E\nu^2, \; \delta = D\nu/w, \; \tilde{\nu} = \tilde{N}\nu/w \qquad \text{(A11)}$$

and assume $E, D, \tilde{N} = O(1)$ (with equation A3, $E \approx 0.28$, $D \approx 0.42\,w$, $\tilde{N} \approx 0.17\,w$). Then a natural boundary layer thickness is ν, and we put

$$y = 1 - \nu Y \qquad \text{(A12)}$$

With $\chi, \psi = O(1)$. The equations are

$$-D\chi_Y + \chi\psi^n + \tilde{N}\psi_Y - (1-\lambda)w + E\psi_{YY} = 0 \qquad \text{(A13a)}$$

$$-\nu\chi\psi^n = [\chi^2(1-\psi_Y)]_Y \qquad \text{(A13b)}$$

At leading order, we find (integrating and matching to the outer solution),

$$\chi^2(1-\psi_Y) \sim \chi_1^2 = (1-\lambda)w \qquad \text{(A14)}$$

We write

$$\psi = u, \quad \psi_Y = 1 - p^2 \qquad \text{(A15)}$$

so that

$$\chi \sim \chi_1/p \qquad \text{(A16)}$$

(and note $p > 0$), and

$$u' = 1 - p^2 \qquad \text{(A17a)}$$

$$p' = \frac{p[\chi_1 u^n + (\tilde{N} - \chi_1^2)p - \tilde{N}p^3]}{2Ep^3 - D\chi_1} \qquad \text{(A17b)}$$

where $' \equiv d/dY$. We seek a trajectory connecting $u = 0$ at $Y = 0$ (since we cannot have $\chi = 0$ there) to $u = \chi_1^{1/n}$, $p = 1$ as $Y \to \infty$. We then find the following. Defining

$$p_0 = (D\chi_1/2E)^{1/3} \qquad \text{(A18)}$$

we have that, if $p_0 < 1$, then $(u,p) = (\chi_1^{1/n}, 1)$ is a stable node or focus. Many trajectories approach the fixed point, possibly oscillatorily, as indicated in Figure A2. This is a rather odd set of solutions, and it is at least plausible that they may be unstable. If $p_0 > 1$, then the fixed point is a saddle, and there is a unique value of p for which the connecting trajectory exists (see Figure A3). Thus a unique, monotonic boundary layer structure exists if

$$E < D\chi_1/2 \qquad \text{(A19)}$$

However, notice that with $E = 0.28$, $D = 0.42$, $\chi_1 \approx 0.9$, this condition would in practice not be satisfied.

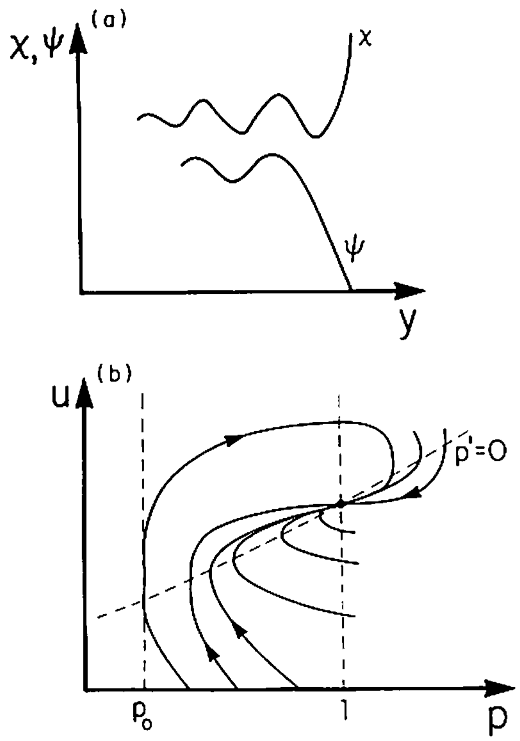

Figure A2. Phase plane and corresponding boundary layer structure near $y = 1$; $E > D\chi_1/2$. A typical solution of the boundary layer equations (A17) is sketched in (b). The approach to the fixed point is oscillatory, giving the spatial variation shown in (a). The melt fraction is horizontally bounded, though the vertical variation is not large. More disquieting is the fact that there are many such solutions, which seems unphysical

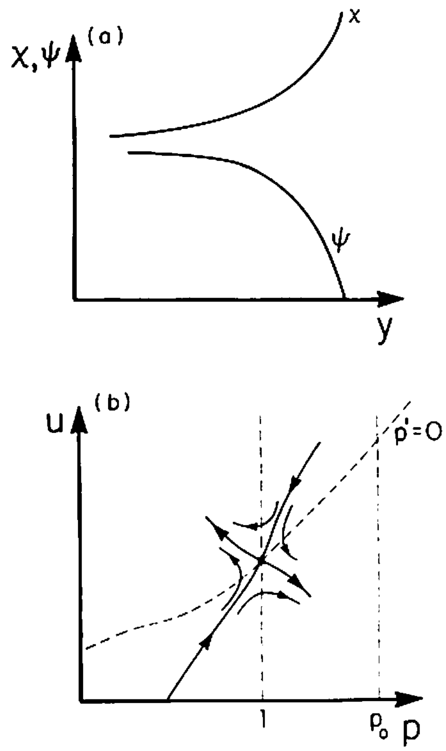

Figure A3. Phase plane and corresponding boundary layer structure near $y = 1$; $E < D\chi_1/2$. As for Figure A2, but when $p_0 > 1$, only one boundary layer solution exists and it is monotonic. Associated with the decrease in effective pressure, the melt fraction increases, though not drastically

Compaction without melting

The last three terms in equation (A1a) are ignored, so that

$$\delta\chi_y + \chi\psi'' = 0 \qquad \text{(A20a)}$$

$$\chi\psi'' = [\chi^2(1 + \nu\psi_y)]_y \qquad \text{(A20b)}$$

where we have put $w = 1$ for simplicity, and we suppose

$$\chi = 1 \text{ at } y = 0 \qquad \text{(A21a)}$$

$$\psi = 0 \text{ at } y = 1 \qquad \text{(A21b)}$$

The outer solution is

$$\chi = \chi_\infty,\ \psi = 0 \qquad \text{(A22)}$$

Integrating once,

$$\delta\chi + \chi^2(1 + \nu\psi_y) = \text{constant} \approx \chi_\infty^2 \qquad \text{(A23)}$$

For the compaction layer, put

$$y = \delta Y,\ \nu = N\delta \qquad \text{(A24)}$$

thus

$$\chi_Y + \chi\psi'' = 0 \qquad \text{(A25a)}$$

$$1 + N\psi_Y \approx \chi_\infty^2/\chi^2 \qquad \text{(A25b)}$$

Now put

$$\chi = e^{-w/2} \qquad \text{(A26)}$$

so that

$$w_Y = 2\psi'' \qquad \text{(A27)}$$

and

$$1 + (N/n2^{1/n})w_Y^{(1/n)-1}w_{YY} = \chi_\infty^2 e^w \qquad \text{(A28)}$$

whence

$$[N/(n+1)2^{1/n}]\,w_Y^{(1/n)+1} = \exp(w - w_\infty) - (w - w_\infty) - 1 \qquad \text{(A29)}$$

where

$$w_\infty = -2 \ln \chi_\infty \tag{A30}$$

Write $Y = [N/(n+1)2^{1/n}]^{n/(n+1)}Z$, so that

$$Z = \int_0^w \frac{dw}{[\exp(w - w_\infty) - (w - w_\infty) - 1]^{n/(n+1)}} \tag{A31}$$

If $n = 1$, then w increases monotonically, and approaches w_∞ exponentially as $Z \to \infty$. If $n > 1$, the approach is algebraic. However, if $n < 1$, then w reaches w_∞ at a finite value of Z, and is identically w_∞ beyond this. Such behaviour is reminiscent of degenerate non-linear diffusion equations, to which (A28) bears some resemblance.

It appears that compaction solutions with arbitrary values of χ_∞ are possible. In particular, an exact solution of the equations is

$$\chi = 1, \ \psi = 0 \tag{A32}$$

It seems that the mathematical model is ill-posed, although the discussion of the thermodynamic boundary conditions in part I suggests that we should choose $\psi = 0$ at $Y = 0$ if $\chi \neq 0$ there, in keeping with equation (A32).

Appendix B: Solitary Waves, Shock Waves

The equations given by Scott and Stevenson (1984) are these:

$$f_t + u_z = 0 \tag{B1a}$$

$$u = f^n[1 + (f^{-m}u_z)_z] \tag{B1b}$$

These equations are also considered by Whitehead and Helfrich (1986), with $m = 1$ and $n = 2$. They admit stable solitary wave solutions, and for small disturbances, Whitehead and Helfrich showed that these were approximately described by the Korteweg–de Vries equation.

To compare this with equation (33), take $\omega = \varepsilon = 0$, and it is convenient (via a rescaling) to take $\lambda = 0$ also. We rescale time as $t = \delta t$, put $\tilde{\nu} = M\delta$ (thus we expect $M = O(1)$). We choose $u_2^s = 1$, and neglect the advective terms of $O(\delta, \tilde{\nu})$ (Scott and Stevenson (1984) do this by moving with the barycentric velocity). In one dimension, the equations are then

$$\chi_t + q_z = 1 + M\psi_t \tag{B2a}$$

$$q = \chi^2[1 + \nu\psi_z] \tag{B2b}$$

$$q_z = \chi|\psi|^{n-1}\psi \tag{B2c}$$

where we write $z = y$. If we choose $n = 1$ in equation (B2), then $\psi = q_z/\chi$, and (B2) is identical with (B1) (with $n = 2$, $m = 1$ there) under the identification $\chi = f$, $q = u$, if z, t in (B2) are rescaled as $z, t \sim \nu^{1/2}$, and if we neglect the right-hand side of (B2a). We leave the scaling as in equation (B2), however. To facilitate comparison, we choose $n = 1$ in equation (B2), so that

$$\chi_t + q_z = 1 + M\frac{\partial}{\partial t}(q_z/\chi) \tag{B3a}$$

$$q = \chi^2[1 + \nu\frac{\partial}{\partial z}(q_z/\chi)] \tag{B3b}$$

We first recall the Whitehead–Helfrich theory, by neglecting the right-hand side of equation (B3a), i.e., we ignore melting. A basic state is then $q = \chi = 1$, and we seek perturbations about this by writing

$$\chi = 1 + \nu\chi_1 + \nu^2\chi_2 \ldots \tag{B4a}$$

$$q = 1 + \nu q_1 + \nu^2 q_2 \ldots \tag{B4b}$$

and we also introduce a second (slow) time-scale τ via $t = \nu\tau$. Equating terms of $O(\nu)$, we have

$$\chi_{1t} + q_{1z} = 0 \tag{B5a}$$

$$q_1 = 2\chi_1 \tag{B5b}$$

whence

$$\chi_1 = A(\zeta,\tau), \ \zeta = z - 2t \tag{B6}$$

which represents a slowly modulated travelling wave. At $O(\nu^2)$,

$$\chi_{2t} + q_{2z} = -A_\tau \tag{B7a}$$

$$q_2 = 2\chi_2 + \chi_1^2 + 2\frac{\partial^2\chi_1}{\partial z^2} \tag{B7b}$$

In order to eliminate secular terms, we require $\chi_{2t} + 2\chi_{2z} = 0$, and thus

$$A_\tau + \frac{\partial}{\partial\zeta}[A^2 + 2A_{\zeta\zeta}] = 0 \tag{B8}$$

which is the Korteweg–de Vries equation.

Let us now repeat the procedure when melting is included. We put $t = \nu\tau$ as before, but now

$$\chi = \chi_0 + \nu\chi_1 + \ldots \tag{B9a}$$

$$q = q_0 + \nu q_1 + \ldots \tag{B9b}$$

and we find

$$q_0 = z, \ \chi_0 = z^{1/2} \quad \text{(B10)}$$

(excluding boundary layer behaviour at $z = 0$). At $O(\nu)$, we find

$$q_1 = 2z^{1/2}\chi_1 - \tfrac{1}{2}z^{-1/2} \quad \text{(B11a)}$$

$$\chi_1 = (1/4z) + \phi \quad \text{(B11b)}$$

where

$$\phi_t + 2(z^{1/2}\phi)_z = 2M\phi_{zt} \quad \text{(B12)}$$

If $M = 0$, this is a recognizable wave equation, but if $M \neq 0$, it is less clear what the behaviour is. So let us first consider $M = 0$, which still includes melting due to heat advection by the rock matrix, but ignores its dependence on p_l. We find at $O(\nu^2)$, that

$$q_2 = 2\chi_0\chi_2 + U \quad \text{(B13a)}$$

$$U = \chi_1^2 - \chi_{1z} + \chi_0 \frac{\partial}{\partial z}(q_{1z}/\chi_0) \quad \text{(B13b)}$$

$$\chi_{2t} + q_{2z} = -\chi_{1\tau} \quad \text{(B13c)}$$

In order to exclude secular terms, we require

$$\chi_{1\tau} + U_z = 0 \quad \text{(B14)}$$

and excluding the steady solution, so $q_1 = 2\chi_0\chi_1$, $\chi_0 = z^{1/2}$, we find from (B12), that

$$\phi = \frac{1}{z^{1/2}} f[z^{1/2} - t; \tau] \quad \text{(B15)}$$

and

$$\phi_\tau + 2\phi\phi_z - \phi_{zz} + \frac{1}{z^{1/2}}\frac{\partial}{\partial z}\left[z^{1/2}\frac{\partial}{\partial z}\left\{ \frac{1}{z^{1/2}}\frac{\partial}{\partial z}(z^{1/2}\phi) \right\}\right] = 0 \quad \text{(B16)}$$

If $M \neq 0$, we can solve equation (B12) using Riemann's representation method. It is more instructive to consider the analogous equation

$$\phi_t + \phi_z = 2M\phi_{zt} \quad \text{(B17)}$$

which has separable solutions $\exp[ikz + \sigma t]$, where

$$\sigma = \frac{2Mk^2 - ik}{1 + 4M^2k^2} \quad \text{(B18)}$$

and thus disturbances grow unstably on the fast time-scale. This suggests that when $M = O(1)$, the expansion scheme is irrelevant, and any disturbances are fundamentally non-linear.

In fact, it is easy to see what then happens (and what happens if $O(1)$ disturbances occur). Going back to equation (B3), we see that when $\chi = O(1)$, the leading order evolution of χ is given by $q = \chi^2$, and thus

$$\chi_t - 2\chi\chi_z = 1 + 2M\chi_{zt} \quad \text{(B19)}$$

Now, if $M = 0$, shocks form, whose structure involves the term in ν, and the shock is of thickness $O(\nu^{1/2})$. If $M \neq 0$, the behaviour of the solutions is unknown. This question is worthy of further investigation.

References

Ahern, J.L. and Turcotte, D.L. (1979). Magma migration beneath an ocean ridge. *Earth Planet. Sci. Lett.*, **45**, 115–122.

Anderson, O.L. and Grew, P.C. (1977). Stress corrosion theory of crack propagation with application to geophysics. *Rev. Geophys. Space Phys.*, **15**, 7–104.

Boulton, G.S. and Hindmarsh, R.C.A. (1987). Sediment deformation beneath glaciers: rheology and geological consequences. *J. Geophys. Res.*, **92**, 9059–9082.

Broek, D. (1986). *Elementary Engineering Fracture Mechanics*. Martinus Nijhoff, Dordrecht, pp. 437.

Emerman, S.H., Turcotte, D.L., and Spence, D.A. (1986). Transport of magma and hydrothermal solutions by laminar and turbulent fluid fracture. *Phys. Earth Planet Inter.*, **41**, 249–259.

Fowler, A.C. (1984). Mantle and magma dynamics. In: *Dynamic Differentiation, Notes of the GFD Summer Program*. Woods Hole Oceanographic Institution, Malkus, W. (ed.) Woods Hole, MA, WHOI 84-44, pp. 74–77.

Fowler, A.C. (1985). A mathematical model of magma transport in the asthenosphere. *Geophys. Astrophys. Fluid Dyn.*, **33**, 63–96.

Fowler, A.C. (1989). Generation and creep of magma in the earth. *SIAM J. Appl. Math.*, **49**, 231–245.

Kushiro, I. (1986). Viscosity of partial melts in the upper mantle. *J. Geophys. Res.*, **91**, 9343–9350.

Marsh, B.D. (1978). On the cooling of ascending andesitic magma. *Philos. Trans. R. Soc. London, Ser. A*, **288**, 611–625.

McKenzie, D.P. (1984). The generation and compaction of partially molten rock. *J. Petrol.*, **25**, 713–765.

McKenzie, D.P. (1985a). ^{230}Th–^{238}U disequilibrium and the melting process beneath ridge axes. *Earth Planet. Sci. Lett.*, **72**, 149–157.

McKenzie, D.P. (1985b). The extraction of magma from the crust and mantle. *Earth Planet Sci. Lett.*, **74**, 81–91.

Miller, R.D. (1980). Freezing phenomena in soils. In Hillel, D. (ed.) *Applications of Soil Physics*. Academic Press, New York, pp. 254–299.

Nicolas, A. (1986). A melt extraction model based on structural studies in mantle peridotites. *J. Petrol.*, **27**, 999–1022.

Nicolas, A. and Jackson, M. (1982). High temperature dikes in peridotites: origin by hydraulic fracturing. *J. Petrol.*, **23**, 568–582.

Olson, P. and Christensen, U. (1986). Solitary wave propagation in a fluid conduit within a viscous matrix. *J. Geophys. Res.*, **91**(B), 6367–6374.

O'Neill, K. and Miller, R.D. (1985). Exploration of a rigid ice model of frost heave. *Water Resour. Res.*, **21**, 281–296.

Ribe, N.M. (1985). The deformation and compaction of partial molten zones. *Geophys. J. R. Astron. Soc.*, **83**, 487–501.

Ribe, N.M. and Smooke, N.D. (1987). A stagnation point flow model for melt extraction from a mantle plume. *J. Geophys. Res.*, **92**, 6437–6443.

Richter, F.M. (1986). Simple models of trace element fractionation during melt segregation. *Earth Planet. Sci. Lett.*, **77**, 333–344.

Richter, F.M. and McKenzie, D.P. (1984). Dynamical models for melt segregation from a deformable matrix. *J. Geol.*, **92**, 729–740.

Röthlisberger, H. (1972). Water pressure in intra- and subglacial channels. *J. Glaciol.*, **11**, 177–203.

Rudnicki, J.W. (1980). Fracture mechanics applied to the earth's crust. *Ann. Rev. Earth Planet. Sci.*, **8**, 489–525.

Ryan, M.P. (1988). The mechanics and three-dimensional internal structure of active magmatic systems: Kilauea volcano, Hawaii. *J. Geophys. Res.*, **93**, 4213–4248.

Ryan, M.P., Koyanagi, R.Y., and Fiske, R.S. (1981). Modeling the three-dimensional structure of macroscopic magma transport systems: application to Kilauea volcano, Hawaii. *J. Geophys. Res.*, **86**, 7111–7129.

Scott, D.R. (1988). The competition between percolation and circulation in a deformable porous medium. *J. Geophys. Res.*, **93**, 6451–6462.

Scott, D.R. and Stevenson, D.J. (1984). Magma solitons. *Geophys. Res. Lett.*, **11**, 1161–1164.

Scott, D.R. and Stevenson, D.J. (1986). Magma ascent by porous flow. *J. Geophys. Res.*, **91**, 9283–9296.

Scott, D.R. and Stevenson, D.J. (1989). A self-consistent model of melting, magma migration and buoyancy-driven circulation beneath mid-ocean ridges. *J. Geophys. Res.*, **94**, 2973–2988.

Scott, D.R., Stevenson, D.J., and Whitehead, J.A. (1986). Observations of solitary waves in a viscously deformable pipe. *Nature*, **319**, 759–761.

Shaw, H.R. (1980). The fracture mechanisms of magma transport from the mantle to the surface. In: Hargraves, R.S. (ed.) *Physics of Magmatic Processes*. Princeton University Press, Princeton, NJ, pp. 201–264.

Sleep, N.H. (1988). Tapping of melt by veins and dykes. *J. Geophys. Res.*, **93**, 10255–10272.

Spera, F.J. (1980). Aspects of magma transport. In: Hargraves, R.B. (ed.) *Physics of Magmatic Processes*. Princeton University Press, Princeton, NJ, pp. 265–323.

Spiegelman, M. and McKenzie, D.P. (1987). Simple 2-D models for melt extraction at mid-ocean ridges and island arcs. *Earth Planet Sci. Lett.*, **83**, 137–152.

Turcotte, D.L. and Ahern, J.L. (1978). A porous flow model for magma migration in the asthenosphere. *J. Geophys. Res.*, **83**, 767–772.

Whitehead, J.A. and Helfrich, K.R. (1986). The Korteweg–de Vries equation from laboratory conduit and magma migration equations. *Geophys. Res. Lett.*, **13**, 545–546.